Anthropogenic and Natural Causes for the Interannual Variation of $PM_{2.5}$ in East Asia During Summer Monsoon Periods From 2008 to 2018

Danyang Ma[1], Min Xie[1,2,*], Huan He[1,2], Tijian Wang[3,*], Mengzhu Xi[1], Lingyun Feng[1], Shuxian Zhang[1], Shitong Chen[1]

[1] School of Environment, Nanjing Normal University, Nanjing 210023, China.

[2] Carbon monitoring and digital application technology center, Carbon peak and carbon neutralization strategy institute of Jiangsu Province, Nanjing 210023, China.

[3] School of Atmospheric Sciences, Nanjing University, Nanjing 210023, China.

Correspondence to: Min Xie(minxie@njnu.edu.cn); Tijian Wang (tjwang@nju.edu.cn)

Abstract. There was a significant difference in near-surface $PM_{2.5}$ across China after the implementation of the Clean Air Action Plan in 2013. This study used the regional climate-chemistry-ecosystem coupled model, RegCM-Chem-YIBs, to investigate interannual variations in $PM_{2.5}$ across East Asia from 2008 to 2018. The drivers of $PM_{2.5}$ variability were examined from Anthropogenic and Natural perspectives. Compared to 2008, $PM_{2.5}$ showed little variation during the PreG phase (2009–2013). However, during the PostG phase (2014–2018), a substantial decline in $PM_{2.5}$ was simulated, particularly in the North China Plain (-36.76 μg/m³) and the Sichuan Basin (-33.96 μg/m³). Anthropogenic pollution emissions were the primary drivers of $PM_{2.5}$ reductions, contributing -10.39 to -3.82 μg/m³ in the PreG period and -33.86 to -8.45 μg/m³ in the PostG period. The influence of meteorological conditions on $PM_{2.5}$ during the PreG phase (-6.31 to 2.32 μg/m³) was comparable to that of anthropogenic pollutant emissions. Additionally, in the vegetation-rich region, the impact of CO_2 emission changes on $PM_{2.5}$ was comparable to that of anthropogenic pollutant emissions. Our study comprehensively examined the drivers of $PM_{2.5}$ concentration changes from 2008 to 2018. We highlight a significant intensification in the contribution of anthropogenic pollutant emissions and reveal that, in regions characterized by dense vegetation, changes in CO_2 concentrations exert a pronounced impact on $PM_{2.5}$ variations.

Graphical Abstract:

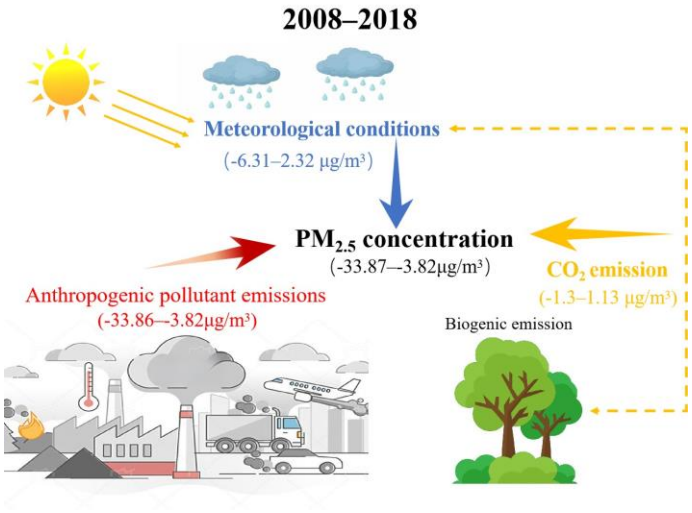

1 Introduction

$PM_{2.5}$ refers to fine particulate matter with an aerodynamic diameter less than or equal to 2.5 micrometers (Chen et al., 2018). Its sources include industrial emissions, vehicular exhaust, biomass burning, and secondary formation from atmospheric gases (Wu et al., 2020). Major chemical components of $PM_{2.5}$ include sulfates, nitrates, ammonium salts, organic carbon, elemental carbon, and heavy metals (Van Donkelaar et al., 2019; Li et al., 2017a). $PM_{2.5}$ is one of the primary atmospheric pollutants in China(Fontes et al., 2017), posing significant risks to human respiratory health(Feng et al., 2016; Xing et al., 2016). Long-term exposure to $PM_{2.5}$ can lead to respiratory diseases such as chronic bronchitis, emphysema, and asthma(Kim et al., 2015; Pui et al., 2014; Xing et al., 2016). Additionally, $PM_{2.5}$ is critical as a short-lived species influencing atmospheric radiation processes(Hu et al., 2017). It affects the radiative energy balance of the Earth-atmosphere system by scattering or reflecting solar radiation (direct effect)(Wu et al., 2021) and altering cloud microphysical properties (indirect effect)(Wang et al., 2018a; Wu et al., 2021).

With China's rapid economic development, widespread $PM_{2.5}$ pollution became prevalent across the country in the early 21st century(Ma et al., 2016). In the most severely polluted urban areas, the annual average $PM_{2.5}$ concentration exceeded 100 $\mu g/m^3$ (Van Donkelaar et al., 2010). From 2000 to 2008, the national average $PM_{2.5}$ concentration in China was 49.4 ± 14.2 $\mu g/m^3$. In eastern China, the average concentration was 55.4 ± 16.1 $\mu g/m^3$, while the Beijing-Tianjin-Hebei region experienced average levels as high as 62.1 ± 22.5 $\mu g/m^3$. The Yangtze River Delta saw an average concentration of 63.0 ± 11.1 $\mu g/m^3$, the Pearl River Delta recorded an average of 52.4 ± 5.8 $\mu g/m^3$, and the Sichuan Basin averaged 61.6 ± 13.4 $\mu g/m^3$ (Wei et al., 2021). To mitigate the severe $PM_{2.5}$ pollution, China implemented the Clean Air Action Plan in 2013(Li et al., 2019). This policy led to a significant nationwide decrease in $PM_{2.5}$ concentrations(Zhang et al., 2019), marking a notable improvement in air quality ever since 2013 (Vu et al., 2019; Li et al., 2018).

The variation in $PM_{2.5}$ concentrations is influenced by three key factors: anthropogenic pollutant emissions, meteorological conditions(Xiao et al., 2021), and Carbon dioxide (CO_2) changes. Anthropogenic pollutant emissions encompass industrial production, transportation, and energy consumption(An et al., 2019), which release amounts of primary $PM_{2.5}$, as well as the precursors of secondary $PM_{2.5}$ such as volatile organic compounds (VOCs) (Kurokawa and Ohara, 2020) and nitrogen oxides (NO_x) (Wu et al., 2020; Zheng et al., 2021a; Kurokawa and Ohara, 2020). Consequently, reducing these emissions is essential for mitigating $PM_{2.5}$ concentrations, as they directly contribute to both the formation and persistence of particulate pollution(Zheng et al., 2018; Zhang et al., 2019).

Meteorological conditions play a significant role in influencing near-surface $PM_{2.5}$ concentrations(Chen et al., 2020b; Xiao et al., 2021). Elevated temperatures can accelerate atmospheric chemical reactions(Mousavinezhad et al., 2021), including oxidation and photochemical processes, thereby promoting the formation of $PM_{2.5}$ (Zhong et al., 2018). In addition, moderate increases in temperature can significantly enhance the emissions of biogenic volatile organic compounds (BVOCs) by stimulating the activity of the synthase enzyme. However, when temperatures exceed the physiological tolerance threshold of plants, decreased enzyme activity or metabolic disruption may suppress emissions(Lindwall et al., 2016; Kleist et al., 2012). Therefore, temperature changes can influence atmospheric $PM_{2.5}$ concentrations by modulating the emissions of BVOCs. Precipitation aids in removing particulate matter from the atmosphere through wet deposition(Zhang et al., 2013), effectively reducing $PM_{2.5}$ pollution

levels (Wu et al., 2018). Additionally, wind speed and direction are crucial factors in the transport and dispersion of particulate matter (Li et al., 2017b). Higher wind speeds facilitate the dispersion of particulate matter over a wider area, reducing its local accumulation and mitigating air pollution in specific regions (Li et al., 2017b; Zhang et al., 2018). The increase in planetary boundary layer height (PBLH) strengthens atmospheric upward motion(Ait-Chaalal et al., 2016), thereby reducing near-surface $PM_{2.5}$ concentrations (Pan et al., 2019).

Changes in CO_2 concentrations can influence $PM_{2.5}$ pollution levels through several mechanisms. Firstly, elevated CO_2 concentrations impact the atmospheric radiation balance, altering the distribution and intensity of precipitation(Cao et al., 2012), which directly affects $PM_{2.5}$ concentrations by influencing wet deposition rates(Zhang et al., 2022). Additionally, Changes in CO_2 concentrations can affect vegetation photosynthesis and growth, which alter the emissions of BVOCs that can participate in atmospheric chemical reactions to form secondary organic aerosols (SOA), and thereby impact atmospheric $PM_{2.5}$ concentrations(Sun et al., 2013; Sun et al., 2012). It is worth noting that elevated CO_2 concentrations may also directly inhibit BVOCs emissions by reducing the activity of BVOCs synthase enzymes(Heald et al., 2009; Pegoraro et al., 2004). Therefore, the impact of increased CO_2 on vegetation BVOCs emissions can be either positive or negative, depending primarily on the relative strength of the inhibitory effect from enzyme suppression versus the stimulatory effect from enhanced photosynthesis(Sun et al., 2012). Isoprene is the most abundant species among BVOCs, so changes in CO_2 concentrations can indirectly affect near-surface $PM_{2.5}$ concentrations by influencing isoprene emissions from vegetation(Sun et al., 2013; Lin et al., 2013; Kramer et al., 2016).

Numerous studies have used statistical models and numerical simulations to investigate the impacts of meteorological conditions and anthropogenic pollution emissions on $PM_{2.5}$ concentration changes in China. The results consistently indicate that changes in anthropogenic pollution emissions are the primary driver of $PM_{2.5}$ variation. Zhang et al. (2019) using the WRF-CMAQ model at the national scale, found that meteorological conditions accounted for only 9 % of the total decline in $PM_{2.5}$ concentrations during 2013–2017 in China, suggesting that emission reductions were the dominant factor. Similarly, based on a multiple linear regression model, Chen et al. (2020a) reported that anthropogenic pollution emission reductions contributed 73 %, 87 %, and 84 % to the $PM_{2.5}$ decline in the North China Plain, Yangtze River Delta, and Pearl River Delta, respectively, while the contribution of meteorological conditions ranged from 10 % to 26 %. Cheng et al. (2019) employing the WRF-CMAQ model, found that the decrease in $PM_{2.5}$ concentrations in Beijing over the same period was mainly attributable to local (65.4 %) and regional (22.5 %) emission reductions, with meteorological conditions accounting for only 12.1 %.

Current research primarily emphasizes the impact of anthropogenic pollutant emissions(Zheng et al., 2018) and meteorological changes on $PM_{2.5}$ concentrations(Zhang et al., 2019; Zhai et al., 2019), while the potential influence of CO_2 concentration changes on $PM_{2.5}$ pollution levels remains largely underexplored. Additionally, following the implementation of the Clean Air Action Plan in 2013, significant decreases in $PM_{2.5}$ concentrations were observed in China. Concurrently, CO_2 levels continued to rise(Xu et al., 2022), with the influence of CO_2 on $PM_{2.5}$ strengthening annually. Therefore, it is essential to analyze the evolution of $PM_{2.5}$ concentrations from 2008 to 2018 in detail, and attribute changes in $PM_{2.5}$ levels to every factor, such as anthropogenic pollution emissions, meteorological conditions, and CO_2 variations.

2 Methods and data

2.1 Model description

In this study, we employed the coupled regional climate-chemistry-ecology model RegCM-Chem-YIBs (Xie et al., 2019; Xie et al., 2024). The RegCM-Chem component simulates key meteorological variables, including temperature, humidity, precipitation, and radiation, along with atmospheric pollutants including ozone and particulate matter (Shalaby et al., 2012). The YIBs (Yale Interactive terrestrial Biosphere) model focuses on simulating vegetation physiological processes, such as ozone-induced damage, photosynthesis, and respiration(Lei et al., 2020). Additionally, it computes important land surface parameters, including CO_2 flux, BVOC emissions, and stomatal conductance (Yue and Unger, 2015). The YIBs model employs a leaf-level BVOC emission scheme based on vegetation photosynthesis. Unlike the traditional MEGAN (Model of Emissions of Gases and Aerosols from Nature) model, this approach incorporates the influence of plant photosynthesis on BVOC emissions, making it more representative of actual plant physiological processes. In this scheme, leaf-level BVOC emission rates depend on the photosynthetic rate, leaf surface temperature, and intracellular CO_2 concentration (Yue and Unger, 2015; Lei et al., 2020; Yue et al., 2015).

The RegCM-Chem and YIBs models exchange variables every 6 minutes, facilitating dynamic coupling between regional climate, atmospheric chemistry, and ecosystem processes. The RegCM-Chem-YIBs model simulated both primary and secondary $PM_{2.5}$ emissions, including dust, black carbon, organic carbon, sulfates, nitrates, and ammonium. The structure of the model is shown in Fig. 1.

In the RegCM-Chem-YIBs model, changes in CO_2 concentrations affect $PM_{2.5}$ primarily via two mechanisms: first, CO_2-induced radiative forcing alters the atmospheric radiation balance, leading to shifts in temperature, precipitation, and boundary‐layer structure that modulate $PM_{2.5}$ formation, transport, and removal(Li and Mölders, 2008; Matthews, 2007); And second, through the YIBs module, changes in CO_2 concentration modulate photosynthetic activity and stomatal behavior, altering BVOCs emissions that undergo atmospheric photochemical oxidation to form secondary organic aerosols, a significant fraction of $PM_{2.5}$ (Kergoat et al., 2002; Kellomaki and Wang, 1998).

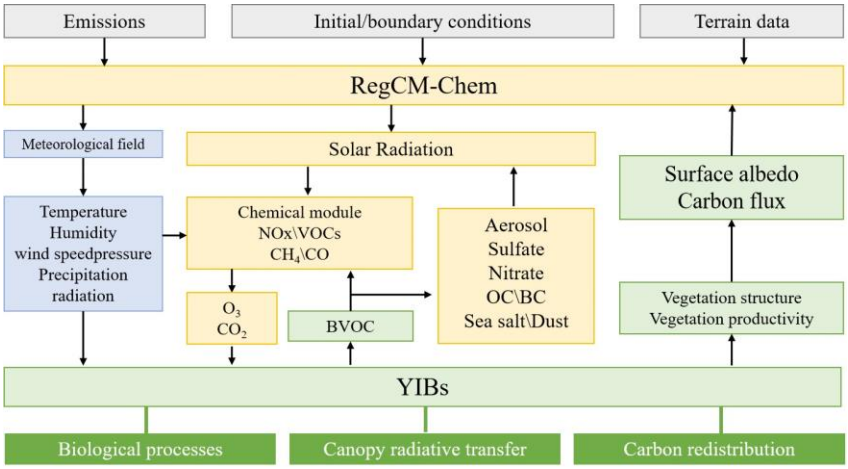

Figure 1. Framework of the RegCM-Chem-YIBs Model.

2.2 Model configurations

The study area covers the entire East Asian region, with a horizontal grid resolution of 60 km, centered at 36°N and 107°E. A terrain-following coordinate system was used vertically(Bleck and Benjamin, 1993), dividing the atmosphere into 18 layers from the surface to 50 hPa.

Anthropogenic pollutant emissions data were obtained from the Multi-resolution Emission Inventory for China (MEIC v1.4) developed by Tsinghua University(Geng et al., 2024). Surface CO_2 flux data were sourced from the National Oceanic and Atmospheric Administration (NOAA) CarbonTracker CT2019 dataset, which includes contributions from fossil fuel combustion, biomass burning, and ocean-atmosphere CO_2 exchange(Peters et al., 2007). Meteorological fields were derived from ERA-Interim reanalysis(Balsamo et al., 2015), while sea surface temperature data were taken from NOAA's weekly mean dataset(Huang et al., 2021). The model employed the Grell cumulus parameterization scheme, CCM3 radiation scheme, Holtslag PBL scheme for boundary layers, CBM-Z mechanism for meteorology and chemistry, and TUV photochemistry scheme.

2.3 Experiment settings

The numerical experiments are presented in Table 1. The SIM_{2008} experiment represents the baseline conditions for the year 2008. In the SIM_{Base} experiment, interannual variations in meteorological fields, CO_2 emissions, and anthropogenic pollutant emissions (excluding CO_2 emissions) were considered for simulations spanning 2009–2018, representing the baseline conditions for 2009–2018. Additionally, the $SIM_{MET=2008}$ and $SIM_{CO2=2008}$ experiments were designed, where meteorological fields and CO_2 emissions were fixed at their 2008 levels, respectively, while simulations were conducted for 2009–2018. The simulation period spans from April to August each year. Among them, the results from May to August, corresponding to the East Asian Summer Monsoon (EASM) period, were selected for analysis.

Changes in $PM_{2.5}$ concentrations were attributed to three main factors: anthropogenic pollution emissions, meteorological conditions, and CO_2 variations. By comparing the simulation results from different years in the SIM_{Base} experiment to SIM_{2008} (SIM_{Base} - SIM_{2008}), we quantified changes in $PM_{2.5}$ concentrations relative to 2008 for the period 2009–2018. To evaluate the impact of meteorological conditions on $PM_{2.5}$ concentrations, we compared the results of the SIM_{Base} experiment with those of the $SIM_{MET=2008}$ experiment for the same year (SIM_{Base} - $SIM_{MET=2008}$). Similarly, the contribution of CO_2 emission changes to $PM_{2.5}$ variations was assessed by comparing the SIM_{Base} experiment with the $SIM_{CO2=2008}$ experiment (SIM_{Base} - $SIM_{CO2=2008}$) in the same year. The contribution of anthropogenic pollutant emissions was then determined by subtracting the effects of meteorological and CO_2 emission changes from the total $PM_{2.5}$ variation.

It is noteworthy that, as a principal greenhouse gas, CO_2 modifies meteorological parameters—such as radiation, temperature, and precipitation—which in turn influence $PM_{2.5}$ levels. In this comparison, all meteorological changes derive solely from variations in CO_2 emissions, a mechanism fundamentally different from the meteorological influences identified in experiments SIM_{Base} and $SIM_{MET=2008}$.

Table 1. The Numerical experimental in this study.

Experiment	Time	Meteorological fields	CO_2 emissions	Anthropogenic pollutant emissions
SIM_{2008}	2008	2008	2008	2008
SIM_{Base}	2009-2018	2009-2018	2009-2018	2009-2018
$SIM_{MET=2008}$	2009-2018	2008	2009-2018	2009-2018
$SIM_{CO2=2008}$	2009-2018	2009-2018	2008	2009-2018

2.4 Model evaluations

Observed $PM_{2.5}$ data were obtained from the China National Environmental Monitoring Center (CNEMC). This study used hourly $PM_{2.5}$ concentrations during the summer monsoon period (May 1 to August 31) from 2015 to 2018. A total of 366 monitoring stations across Chinese cities, selected based on data completeness and representativeness, were used for model validation. The locations of these stations are shown in Fig. S5. CO_2 observations were sourced from the World Data Centre for Greenhouse Gases (WDCGG), including all seven sites in East Asia: Waliguan, Korea Tae-ahn Peninsula, Ulaanbaatar in Mongolia, Lulin, Yonagunijima, Cape D'Aguilar (Hong Kong), and King's Park. Detailed station locations are shown in Fig. S6. Reanalysis data for temperature, wind fields, and relative humidity were obtained from the ERA-Interim dataset.

As shown in Table 2 and Figures S1–S6, the SIM_{Base} experiments reproduce 2015–2018 $PM_{2.5}$ and CO_2 concentrations with high correlations and low biases relative to observations, while their simulated meteorological fields closely match reanalysis data. Overall, the RegCM-Chem-YIBs model effectively captures the fundamental characteristics and temporal trends of meteorological factors, $PM_{2.5}$, and CO_2 concentrations in East Asia(Ma et al., 2023a; Ma et al., 2023b).

Table 2. Evaluations of the near-surface CO_2 and $PM_{2.5}$ in East Asia.

Species	Year	Observation	Simulation	Bias	RMSE	R
CO_2（ppm）	2015	402.82	406.98	4.16	9.37	0.44
	2016	407.12	410.44	3.32	8.22	0.69
	2017	408.35	413.62	5.27	11	0.39
	2018	409.61	416.68	7.07	11.32	0.41
$PM_{2.5}$ （ug/m^3）	2015	36.6	25.57	-11.03	12.99	0.71
	2016	31.03	22.91	-8.12	10.31	0.64
	2017	29.61	24.02	-5.59	10.57	0.71
	2018	27.18	19.04	-8.14	11.62	0.61

RMSE: root mean square error; R: correlation coefficient.

3 Results and discussion

3.1 $PM_{2.5}$ variation

Changes in $PM_{2.5}$ concentrations from 2009 to 2018 relative to 2008 were quantified by

comparing simulation results from each year in the SIM_{Base} experiment with SIM_{2008} (SIM_{Base} - SIM_{2008}). Figure 2 illustrates the changes in near-surface $PM_{2.5}$ concentrations across East Asia from 2009 to 2018. $PM_{2.5}$ concentrations are notably higher in the North China Plain, northeastern China, and eastern China (Shanghai, Jiangsu, Zhejiang), largely driven by industrial emissions, vehicle exhaust, coal combustion, and dust from human activities(Wang et al., 2017). In contrast, regions in western China (Yunnan, Gansu, Xinjiang) exhibit lower $PM_{2.5}$ levels due to limited industrial activity, lower population density, and more favorable meteorological conditions (Low water vapor content, lower temperatures, and weak solar radiation are unfavorable for the formation of secondary aerosols such as sulfates, nitrates, and organic aerosols)(Wei et al., 2021; Xue et al., 2020). Developed cities and industrial centers like the Pearl River Delta and Fuzhou (Fujian Province) continue encountering challenges related to $PM_{2.5}$ pollution. Moreover, the Sichuan region, characterized by its enclosed basin geography and high population density, also experiences high $PM_{2.5}$ pollution levels(Wang et al., 2018b). From 2009 to 2013, $PM_{2.5}$ concentrations in China remained relatively stable, with levels averaging around 90 μg/m³ in the North China Plain and Sichuan Basin. However, following the implementation of the Clean Air Action Plan in 2013, $PM_{2.5}$ levels significantly declined nationwide. By 2018, concentrations had dropped to below 50 μg/m³ across much of the country.

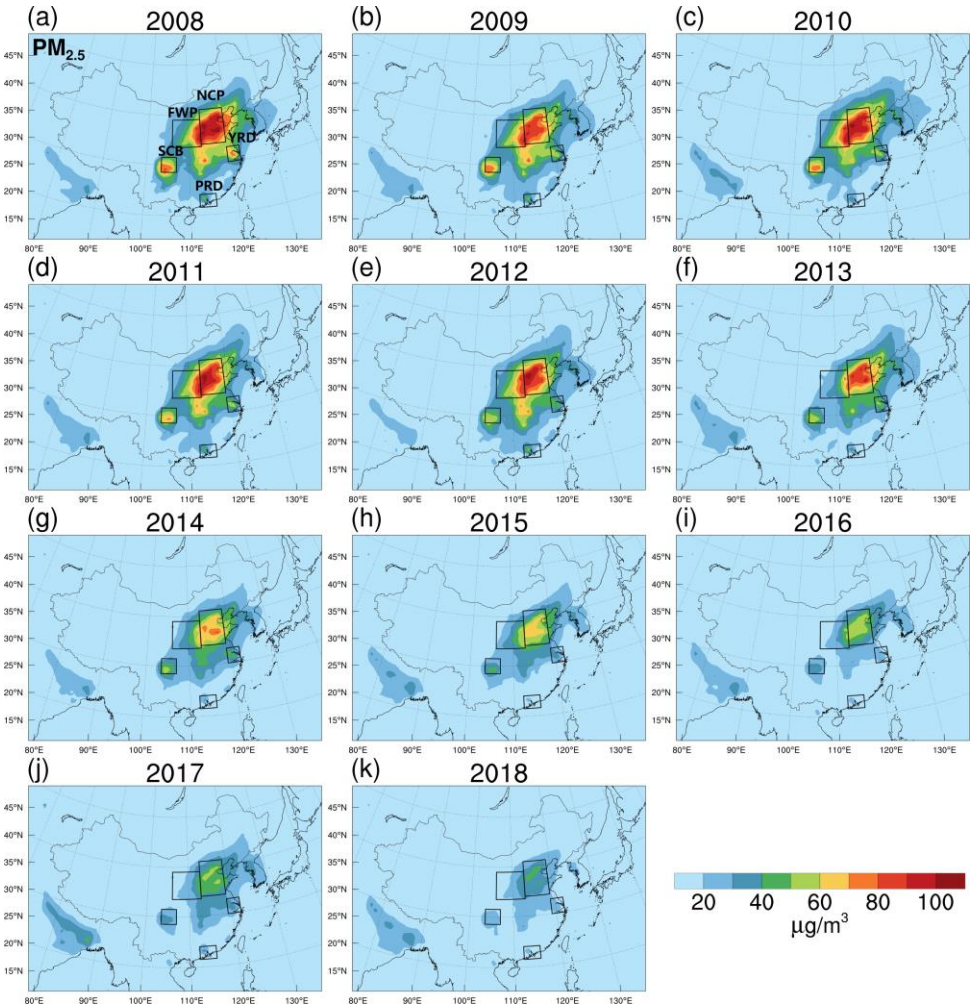

Figure 2. Near-surface $PM_{2.5}$ concentrations (μg/m³) over East Asia during the EASM period from 2009 (a) to

2018 (k) (SIM_{2008}). Key regions are highlighted by black boxes, including the North China Plain (NCP), Fenwei Plain (FWP), Yangtze River Delta (YRD), Pearl River Delta (PRD), and Sichuan Basin (SCB).

Figure 3 and Table 3 present the changes in $PM_{2.5}$ concentrations relative to 2008 across East Asia from 2009 to 2018. Since 2008, most regions in China have seen varying degrees of $PM_{2.5}$ reduction. During the pre-governance period (PreG, 2009~2013), the largest decrease occurred in the Yangtze River Delta, with a reduction of 14.77 μg/m³, followed by the Sichuan Basin and Pearl River Delta, where concentrations dropped by 10.59 μg/m³ and 8.69 μg/m³, respectively. In contrast, the Fenwei Plain and Pearl River Delta experienced smaller changes, with reductions of less than 3 μg/m³. $PM_{2.5}$ concentrations across China significantly decreased after the implementation of the Clean Air Action Plan in 2013. The most notable reductions were simulated in the North China Plain and Sichuan Basin, where $PM_{2.5}$ concentrations dropped by 36.76 μg/m³ and 33.96 μg/m³, respectively. In the Fenwei Plain and Yangtze River Delta, $PM_{2.5}$ concentrations decreased by 22.16 to 27.89 μg/m³. In contrast, the Pearl River Delta saw a smaller reduction, with levels decreasing by just 8.03 μg/m³. This may be attributed to the region's significant influence from the summer monsoon and relatively lower impact from anthropogenic pollution emissions. Further analysis of these factors will be conducted in subsequent sections.

Table S1 shows that the mean $PM_{2.5}$ trend over China during the PreG (2009-2013) and PostG (2014-2018) periods was −1.84 $\mu g/m^3$/yr and −2.90 $\mu g/m^3$/yr, respectively. These values are consistent with the findings of Silver et al. (2025), who reported a $PM_{2.5}$ trend of −2.47 $\mu g/m^3$/yr for 2014–2017 in China based on ground-based observations. Similarly, Lin et al. (2018) reported $PM_{2.5}$ trends of −0.65 and −2.30 $\mu g/m^3$/yr for 2006–2010 and 2011–2015 in China, respectively. Using satellite remote sensing data, Ma et al. (2019) found declines of 1.03 and 4.27 $\mu g/m^3$/yr for 2010-2013 and 2013-2017 in China, respectively. The high-resolution Chinese air quality reanalysis (CAQRA), developed by Kong et al. (2021) using data assimilation techniques, indicated a more pronounced decline of −5.80 $\mu g/m^3$/yr for $PM_{2.5}$ from 2013 to 2018 in China. In addition, Silver et al. (2018), based on multi-source data, reported a trend of −3.40 $\mu g/m^3$/yr for 2015–2017 in China. Therefore, our simulation accurately captures the observed $PM_{2.5}$ trends over China from 2008 to 2018, providing a robust foundation for subsequent attribution analyses.

Overall, before 2013, near-surface $PM_{2.5}$ concentrations across China showed little variation. However, after 2013, a significant reduction in $PM_{2.5}$ pollution levels was simulated nationwide. Changes in $PM_{2.5}$ concentrations were attributed to three main factors: anthropogenic pollution emissions, meteorological conditions, and CO_2 variations. The following sections analyze each factor’s contribution to the changes in $PM_{2.5}$ concentrations from 2008 to 2018.

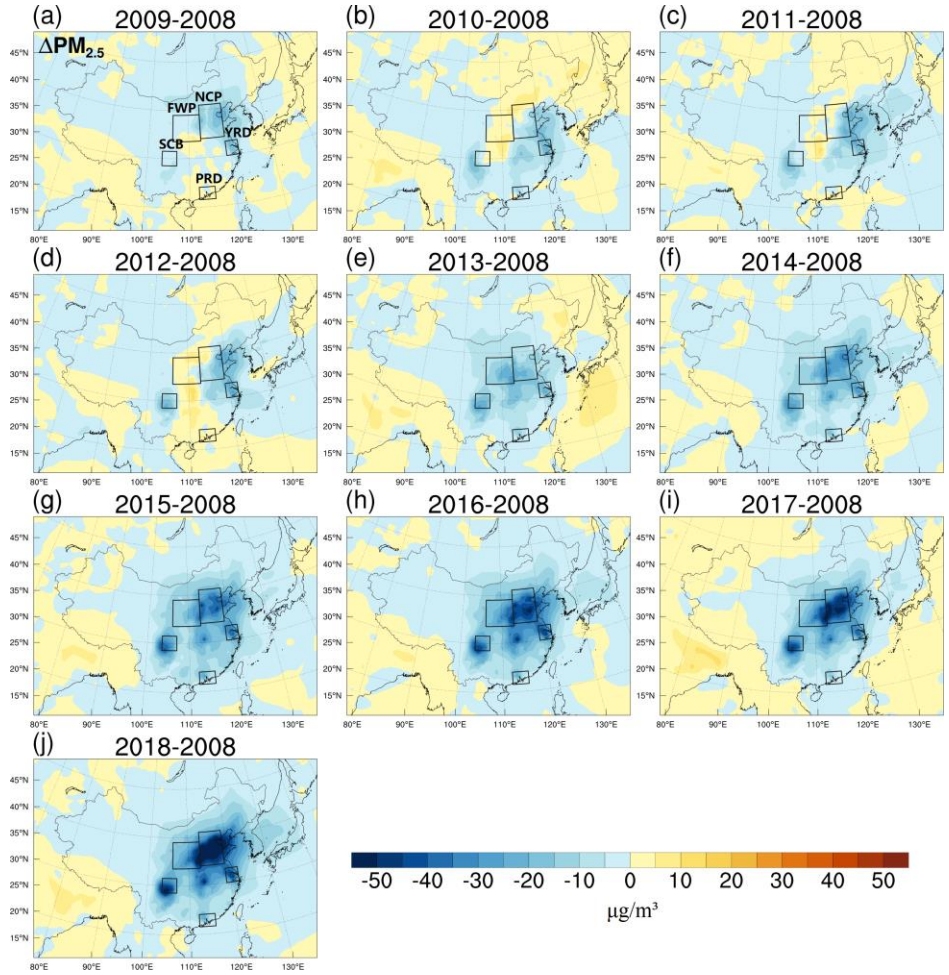

Figure 3. Changes in near-surface $PM_{2.5}$ concentrations (μg/m³) during the EASM period from 2009 (a) to 2018 (j) relative to 2008 in East Asia (SIM_{Base} - SIM_{2008}).

Table 3. Changes in near-surface $PM_{2.5}$ concentrations (μg/m³) during the EASM period from 2009 to 2018 relative to 2008 in the North China Plain (NCP), Fen-Wei Plain (FWP), Yangtze River Delta (YRD), Pearl River Delta (PRD), and Sichuan Basin (SCB) (SIM_{Base} - SIM_{2008}).

Year	NCP	FWP	YRD	PRD	SCB
2009	-11.24	-1.29	-11.37	1.41	-3.16
2010	-3.87	1.9	-15.2	-3.57	-4.79
2011	-6.27	0.22	-14.76	0.13	-8.65
2012	-7.42	1.69	-17.61	2.35	-15.99
2013	-14.67	-15.49	-14.9	-6.34	-20.37
2014	-24.26	-15.36	-19.95	-6.72	-22.87
2015	-31.41	-16.9	-27.76	-9.91	-31.75
2016	-38.5	-25.23	-32.43	-8.18	-35.58
2017	-40.69	-25.49	-26.21	-5.82	-37.43
2018	-48.96	-27.83	-33.08	-9.53	-42.19
PreG	-8.69	-2.59	-14.77	-1.20	-10.59
PostG	-36.76	-22.16	-27.89	-8.03	-33.96

3.2 Contribution of meteorological conditions

The impact of meteorological conditions variations on $PM_{2.5}$ concentrations were assed by compared SIM_{Base} results with those from $SIM_{MET=2008}$ for the same year (SIM_{Base} - $SIM_{MET=2008}$). As shown in Fig. 4, during the PreG period, the precipitation increased by 2–4 mm/day in China's eastern coastal and western inland regions, while it decreased by approximately 2 mm/day in central China. This increase in precipitation facilitates the reduction of near-surface $PM_{2.5}$ concentrations through wet deposition. Consequently, trends in $PM_{2.5}$ concentrations are inversely related to precipitation: concentrations decreased by 2–16 $\mu g/m^3$ in the eastern coastal and western inland regions, while increased by 4–8 $\mu g/m^3$ around 110°E in central China. Additionally, in northeastern and southwestern China, wind speeds increased by 1 to 2 m/s, contributing to the reduction of $PM_{2.5}$ concentrations. In contrast, decreased wind speeds in southeastern and central China facilitated the accumulation of $PM_{2.5}$. During the PostG period, the significant increase in temperature (Fig. 4l) promoted the formation of $PM_{2.5}$, leading to an expansion of the areas where $PM_{2.5}$ concentrations increased. Overall, $PM_{2.5}$ concentrations have decreased in the eastern coastal and western inland regions but increased in the central area of China.

Table 4 indicates that in the NCP region, precipitation increased by 0.58 to 0.6 mm/day, and wind speed rose by 0.17 to 0.26 m/s during the PreG and PostG periods, resulting in a decrease in near-surface $PM_{2.5}$ concentrations of 1.6 to 4.01 $\mu g/m^3$. In the FWP region, $PM_{2.5}$ concentrations increased by 1 to 2.31 $\mu g/m^3$, which was associated with a rise in temperature of 0.1 to 0.46 K and a significant decrease in PBLH of 108.5 to 15.3 m. In the YRD region, the increase in wind speed of 0.48 to 1.02 m/s facilitated a reduction in $PM_{2.5}$ concentrations by 0.43 to 0.61 $\mu g/m^3$. Conversely, in the PRD region, reduced precipitation combined with increased temperature contributed to an increase in $PM_{2.5}$ concentrations, ranging from 0.11 to 1.49 $\mu g/m^3$. In the SCB region, $PM_{2.5}$ concentrations rose by 0.29 $\mu g/m^3$ during the PreG period, linked to a significant decrease in PBL height of 136.5 m. In the PostG period, $PM_{2.5}$ concentrations decreased by 1.14 $\mu g/m^3$, attributed to an increase in precipitation (0.37 mm/day) and a decrease in temperature (0.14 K).

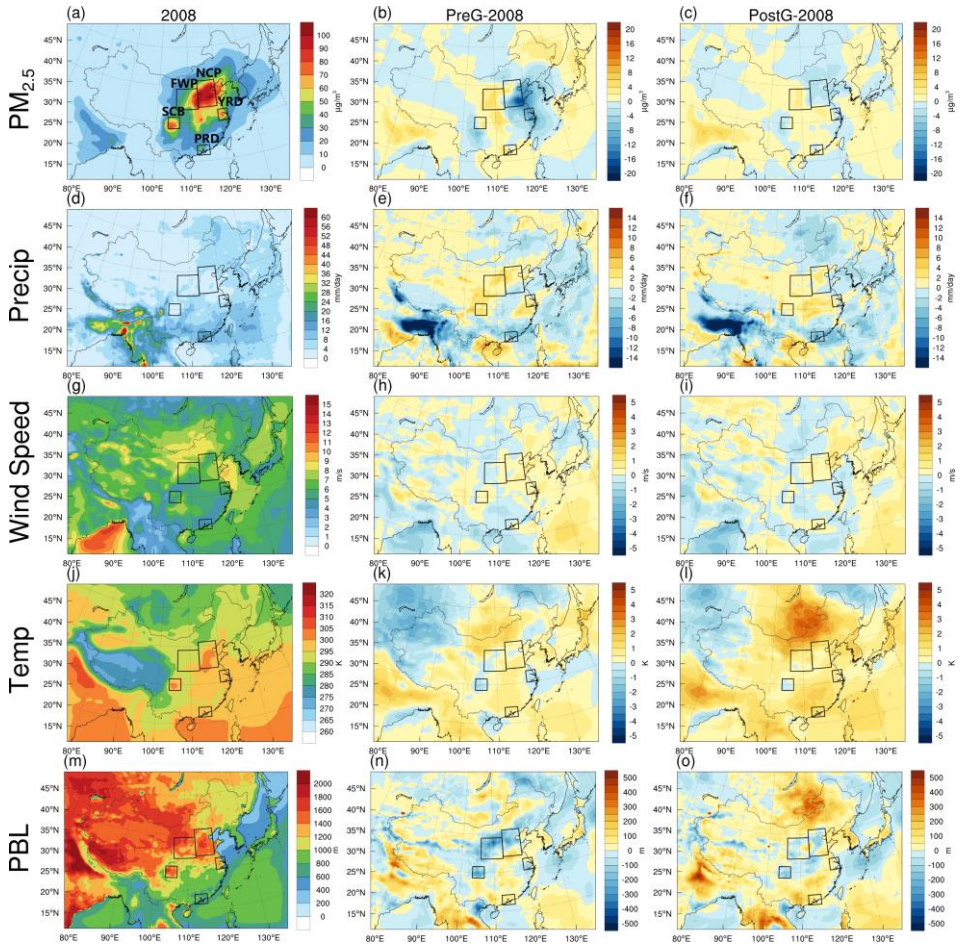

Figure 4. The $PM_{2.5}$ (a–c, μg/m³), precipitation (d–f, mm/day), wind speed (g–i, m/s), temperature (j–l, K), and Planetary Boundary Layer (PBL) height (m–o, m) during the EASM period in 2008 (left), and their mean changes due to meteorological variations in PreG (2009–2013, center) and PostG (2014–2018, right) phase relative to 2008 (SIM_{Base} - $SIM_{MET=2008}$).

Table 4. Impact of meteorological condition changes on $PM_{2.5}$ (μg/m^3), precipitation (mm/day), wind speed (m/s), near-surface temperature (K), and Planetary Boundary Layer (PBL) height (m) during the EASM period in PreG (2009–2013) and PostG (2014–2018) phase relative to 2008 (SIM_{Base} - $SIM_{MET=2008}$).

Region	Period	$PM_{2.5}$ (μg/m^3)	Precipitation (mm/day)	Wind Speed (m/s)	Near-Surface Temperature (K)	PBL (m)
NCP	PreG	-4.01	0.58	0.17	0.32	-46.8
	PostG	-1.6	0.6	0.26	0.6	-14.5
FWP	PreG	2.32	1.68	-0.06	0.1	-108.5
	PostG	1	0.81	0.05	0.46	-15.3
YRD	PreG	-6.31	1.02	0.18	-0.29	-33.9
	PostG	-0.43	0.48	-0.08	0.45	21.9
PRD	PreG	1.49	-2.39	-0.02	0.36	29.6
	PostG	0.11	-3.24	0.18	1.00	52.2
SCB	PreG	0.29	1.81	0.13	-0.58	-136.5
	PostG	-1.14	0.37	-0.03	-0.14	-76

3.3 Contribution of CO_2

The contribution of CO_2 emission changes to $PM_{2.5}$ variability was quantified by comparing the SIM_{Base} experiment with the $SIM_{CO2=2008}$ experiment (SIM_{Base} - $SIM_{CO2=2008}$) within the same year. As shown in Fig. 5, Following the ongoing urbanization and industrialization, CO_2 concentrations across East Asia rose by 2–10 ppm during both the PreG and PostG periods, with a sharper increase in the PostG period. CO_2 influences atmospheric $PM_{2.5}$ concentrations both through its radiative effects on precipitation and by altering BVOCs emissions from vegetation. Overall, CO_2 changes contributed to $PM_{2.5}$ variations across East Asia from 2008 to 2018, ranging from -4 to 6 μg/m³. $PM_{2.5}$ pollution levels generally increased in the PreG period, while reductions were more common in the PostG period.

Table 5 presents a detailed analysis of the five target regions. In northern China, particularly the NCP and FWP regions, limited vegetation coverage means CO_2 impacts surface $PM_{2.5}$ concentrations mainly through precipitation changes. In the PostG period, precipitation increased by 0.06–0.13 mm/day, lowering $PM_{2.5}$ concentrations by 0.98–1.3 μg/m^3. Similarly, in the Sichuan Basin, precipitation rose by 0.21–0.64 mm/day, reducing $PM_{2.5}$ concentrations by 0.49–0.73 μg/m^3 in the PreG and PostG period. However, in the YRD and PRD regions, where vegetation coverage is higher, CO_2 primarily impacts $PM_{2.5}$ concentrations by modulating BVOCs emissions. The impact can be either positive or negative(Possell et al., 2005), depending primarily on the balance between the inhibitory effects on synthase activity and the stimulatory effects of enhanced photosynthesis(Wilkinson et al., 2009). In the YRD region, isoprene fell by 0.32–0.58 μg/m^3 during both periods, while precipitation rose by 0.09–0.13 mm/day, collectively reducing $PM_{2.5}$ by 0.02–0.05 μg/m³. In the PRD region, isoprene concentrations increased significantly by 0.31–0.92 μg/m³, while precipitation decreased by 0.33–1.02 mm/day. Consequently, $PM_{2.5}$ concentrations rose by 0.31–1.13 μg/m³ during both the PreG and PostG periods.

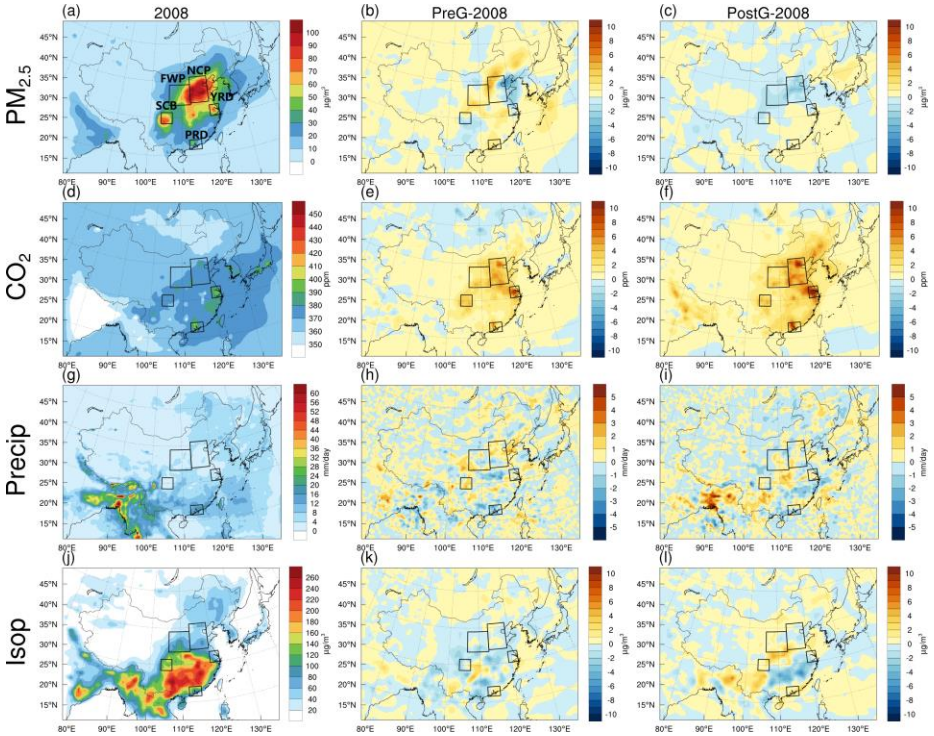

Figure 5. The $PM_{2.5}$ (a–c, μg/m³), CO_2 (d–f, ppm), precipitation (g–i, mm/day), and isoprene (j–l, μg/m³) during the EASM period in 2008 (left), and their mean changes due to CO_2 emission variations in PreG (2009–

2013, center) and PostG (2014–2018, right) phase relative to 2008 (SIM_{Base} - $SIM_{CO2=2008}$).

Table 5. Impact of CO_2 emission changes on $PM_{2.5}$ (μg/m^3), CO_2 (ppm), precipitation (mm/day), and isoprene (μg/m^3) during the EASM period in PreG (2009–2013) and PostG (2014–2018) phase relative to 2008 (SIM_{Base} - $SIM_{CO2=2008}$).

Region	Period	$PM_{2.5}$ (μg/m^3)	CO_2 (ppm)	Precipitation (mm/day)	Isoprene (μg/m^3)
NCP	PreG	0.6	3.19	0.27	-0.1
	PostG	-1.3	4.24	0.13	0.26
FWP	PreG	0.84	1.70	0.21	-0.16
	PostG	-0.98	2.05	0.06	0.33
YRD	PreG	-0.02	4.1	0.13	-0.32
	PostG	-0.05	6.2	0.09	-0.58
PRD	PreG	1.13	1.97	-1.02	0.31
	PostG	0.31	3.20	-0.33	0.92
SCB	PreG	-0.49	2.80	0.64	-0.78
	PostG	-0.73	2.78	0.21	0.69

3.4 Contribution of anthropogenic pollutant emissions

The contribution of changed anthropogenic pollutant emissions to $PM_{2.5}$ variation was determined by removing the effects of meteorological and CO_2 emission changes from the total variation. Figure 6 illustrates a significant downward trend in $PM_{2.5}$ concentrations across East Asia since 2008. During the PreG period, $PM_{2.5}$ levels decreased by an average of 5 to 10 μg/m^3 over East Asia. Following the implementation of the Clean Air Action Plan in 2013, a marked reduction in $PM_{2.5}$ concentrations was simulated. The most substantial decreases occurred in the NCP and SCB region, with approximately 60 μg/m³. Anthropogenic pollutant emissions emerged as the primary drivers of this decline, with their spatial distribution and magnitude of impact closely corresponding to the overall changes in $PM_{2.5}$ concentrations. In contrast, the effects of changing meteorological conditions and CO_2 emissions on $PM_{2.5}$ levels in East Asia were relatively minor, ranging between -5 to 5 μg/m³. Meteorological conditions have reduced $PM_{2.5}$ concentrations in the eastern coastal and western regions of China, while increasing them in the central region. In the PostG period, the extent of $PM_{2.5}$ concentration increases has expanded. The impact of CO_2 emission changes on $PM_{2.5}$ levels shows different trends in the PreG and PostG periods. In the PreG period, changes in CO_2 emissions primarily led to an increase in $PM_{2.5}$ concentrations. However, in the PostG period, the rise in CO_2 concentrations began to have a negative impact, leading to a reduction in $PM_{2.5}$ concentrations.

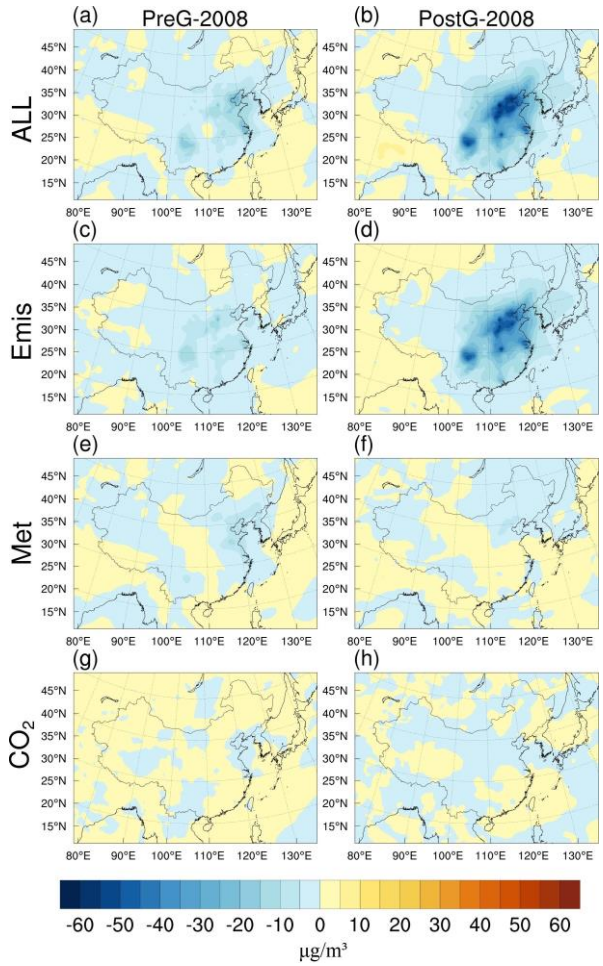

Figure 6. The total changes in $PM_{2.5}$ concentrations (All, SIM_{Base} - SIM_{2008}), and the changes in $PM_{2.5}$ attributed to variations of anthropogenic pollutant emissions (Emis, All-Met-CO_2), meteorological conditions (Met, SIM_{Base} – $SIM_{MET=2008}$), and CO_2 emissions (CO_2, SIM_{Base} - $SIM_{CO2=2008}$) during the EASM period in PreG (2009–2013, left) and PostG (2014–2018, right) phase relative to 2008.

Based on Fig. 7 and Table 6, $PM_{2.5}$ concentrations in the NCP region decreased by 5.28 μg/m³ during the PreG period and by 33.86 μg/m³ in the PostG period. Anthropogenic pollution emissions were the primary driver of these changes. During the PreG period, the influence of meteorological conditions on $PM_{2.5}$ was comparable to that of anthropogenic pollution emissions, with changes in meteorology contributing -4.01 μg/m³ and emissions contributing -5.28 μg/m³. However, in the PostG period, the impact of meteorological factors diminished to -1.6 μg/m³, indicating that anthropogenic pollution emissions became the predominant factor in the reduction of $PM_{2.5}$ concentrations. In contrast, the effect of changes in CO_2 emissions on $PM_{2.5}$ levels was relatively minor, ranging from -1.3 to 0.6 μg/m³.

The situation in the FWP region is similar to that of the NCP region, with anthropogenic pollution emissions as the primary driver of reduced $PM_{2.5}$ concentrations. During the PreG and PostG periods, the contributions of anthropogenic pollution emissions to $PM_{2.5}$ levels were -5.75 μg/m³ and -22.18 μg/m³, respectively. In contrast, meteorological conditions contributed to an increase in $PM_{2.5}$ concentrations, with a contribution of 2.32 μg/m³ in the PreG period, comparable to the impact of anthropogenic pollution emissions. Meanwhile, the influence of CO_2 emissions on $PM_{2.5}$ levels was relatively minor.

In the YRD region, anthropogenic pollution emissions are the primary driver of reduced $PM_{2.5}$ concentrations. Due to its location in eastern China, the YRD region is more affected by the EASM, resulting in more pronounced effects of changing meteorological conditions on $PM_{2.5}$ levels compared to the NCP and FWP regions. During the PreG period, the impact of meteorological conditions on $PM_{2.5}$ concentrations reached as high as -6.31 μg/m³.

In the PRD region, changes in anthropogenic pollution emissions have contributed to a reduction in $PM_{2.5}$ concentrations, ranging from -8.45 to -3.82 μg/m³. However, changes in meteorological conditions and CO_2 emissions have led to increases in $PM_{2.5}$ levels, ranging from 0.11 to 1.49 μg/m³. Similar to the YRD region, the effects of changing meteorological conditions on $PM_{2.5}$ concentrations are significant, peaking at 1.49 μg/m³ during the PreG period. Located in southeastern coastal China, the Pearl River Delta's rich vegetation cover enhances the impact of CO_2 emission changes on $PM_{2.5}$ concentrations. During the PreG period, the influence of CO_2 emission changes on $PM_{2.5}$ levels reached 1.13 μg/m³, comparable to the effect of anthropogenic pollution emissions (-3.82 μg/m³). In the PostG period, the impact of CO_2 emission changes (0.31 μg/m³) surpassed that of meteorological conditions (0.11 μg/m³).

In the SCB region, the basin topography results in relatively minor effects of meteorological conditions and CO_2 emission changes on $PM_{2.5}$ levels, with contributions ranging from -1.14 to 0.29 μg/m³ during both the PreG and PostG periods. In contrast, anthropogenic pollution emissions are the primary drivers of reduced $PM_{2.5}$ concentrations, exerting an impact of -32.09 μg/m³ during the PostG period.

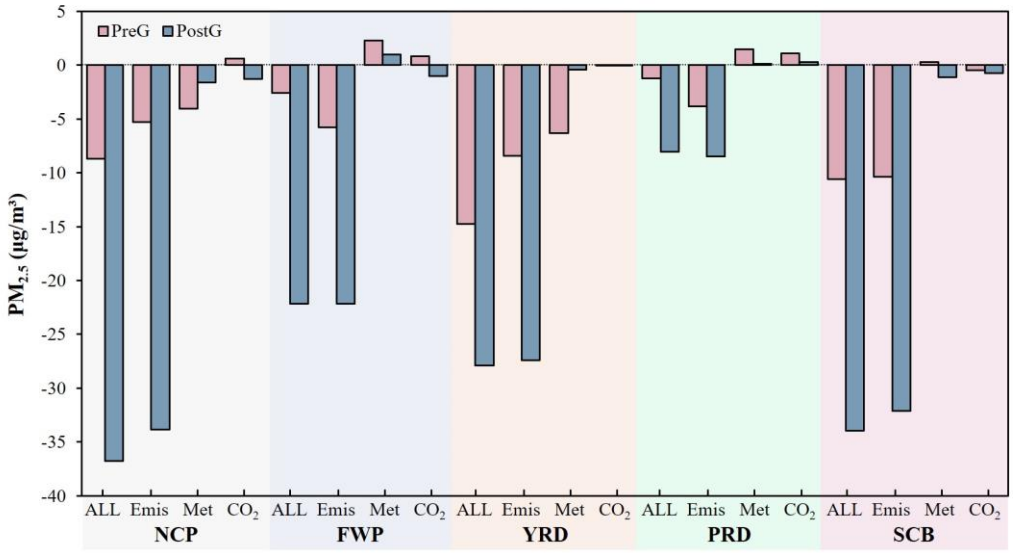

Figure 7. The total changes in $PM_{2.5}$ concentrations (All, SIM_{Base} - SIM_{2008}) for the North China Plain (NCP), Fenwei Plain (FWP), Yangtze River Delta (YRD), Pearl River Delta (PRD), and Sichuan Basin (SCB) during the EASM period in PreG (2009–2013) and PostG (2014–2018) phase relative to 2008, along with the variations in $PM_{2.5}$ due to anthropogenic pollutant emissions (Emis, All-Met-CO_2), meteorological conditions (Met, SIM_{Base} – $SIM_{MET=2008}$), and CO_2 emission (CO_2, SIM_{Base} - $SIM_{CO2=2008}$) changes.

Table 6. Changes in total $PM_{2.5}$ concentrations (ALL, SIM_{Base} - SIM_{2008}) and the impacts of anthropogenic pollutant emissions (Emis, All-Met-CO_2), meteorological conditions (Met, SIM_{Base} - $SIM_{MET=2008}$), and CO_2

emission (CO_2, SIM_{Base} - $SIM_{CO2=2008}$) variations on $PM_{2.5}$ concentrations ($\mu g/m^3$) during the EASM period in PreG (2009–2013) and PostG (2014–2018) phase relative to 2008.

Region	Period	ALL	Emis	Met	CO_2
NCP	PreG	-8.69	-5.28	-4.01	0.6
	PostG	-36.76	-33.86	-1.6	-1.3
FWP	PreG	-2.59	-5.75	2.32	0.84
	PostG	-22.16	-22.18	1	-0.98
YRD	PreG	-14.77	-8.44	-6.31	-0.02
	PostG	-27.89	-27.41	-0.43	-0.05
PRD	PreG	-1.2	-3.82	1.49	1.13
	PostG	-8.03	-8.45	0.11	0.31
SCB	PreG	-10.59	-10.39	0.29	-0.49
	PostG	-33.96	-32.09	-1.14	-0.73

3.5 Attribution of Changes in $PM_{2.5}$

Figure 8 illustrates that $PM_{2.5}$ concentrations remained relatively stable across the five regions during the PreG period. However, in the PostG period, following the implementation of the Clean Air Action Plan, significant reductions in $PM_{2.5}$ concentrations were simulated in the NCP, FWP, YRD, and SCB regions, while the PRD region showed the smallest decrease.

Anthropogenic pollutant emissions are the primary factor driving $PM_{2.5}$ concentration reductions across the five regions, with their impact increasing linearly over time. In the PreG period, meteorological conditions had a relatively stronger influence on $PM_{2.5}$ levels, occasionally surpassing the effects of anthropogenic pollution emissions. For example, in 2013, the meteorological and emission impacts on $PM_{2.5}$ in the NCP region were -17.35 $\mu g/m^3$ and 4.49 $\mu g/m^3$, respectively. Similarly, in the FWP region from 2013 to 2015, meteorological impacts ranged from -16.9 to -15.36 $\mu g/m^3$, while emissions affected $PM_{2.5}$ concentrations between -15.8 and -2.27 $\mu g/m^3$. The influence of meteorology also exceeded that of emissions in the YRD region during 2011–2012 and in the PRD region in 2010. Even in the SCB region, where meteorological impacts on $PM_{2.5}$ were relatively minor, meteorological effects in 2010 (8.59 $\mu g/m^3$) were comparable to emissions (-14.67 $\mu g/m^3$).

The influence of CO_2 emission changes on $PM_{2.5}$ levels was generally minor but, in the densely vegetated PRD region, could be comparable to the effects of emissions and meteorology. The influences of CO_2 emissions, anthropogenic pollutant emissions, and meteorology on $PM_{2.5}$ are -0.25 to 3.11 $\mu g/m^3$, -6.19 to -1.47 $\mu g/m^3$, and -0.5 to 3.11 $\mu g/m^3$, respectively from 2009 to 2013.

Our attribution analysis of $PM_{2.5}$ concentration changes is mainly consistent with previous studies, which have indicated that variations in anthropogenic pollution emissions were the primary driver of $PM_{2.5}$ changes in China during 2013-2017, with meteorological conditions contributing approximately 9 %-26 % (Zhang et al., 2019; Chen et al., 2020a; Cheng et al., 2019). In our study, relative to 2008, the average contribution of anthropogenic pollution emissions during the PreG period was 89.08 %, while meteorological conditions contributed 16.45 %. In the PostG period, following the implementation of the Clean Air Action Plan, the influence of anthropogenic pollution emissions further increased to 96.26 %, whereas the contribution of meteorological conditions declined to 1.60 %. This finding underscores that the impact of changes in anthropogenic pollution emissions on $PM_{2.5}$ concentrations was markedly enhanced

after 2013. Notably, changes in CO_2 emissions had a significant impact on $PM_{2.5}$ levels, contributing -5.46 % during the PreG period and 2.14 % during the PostG period, with the latter effect surpassing that of meteorological conditions.

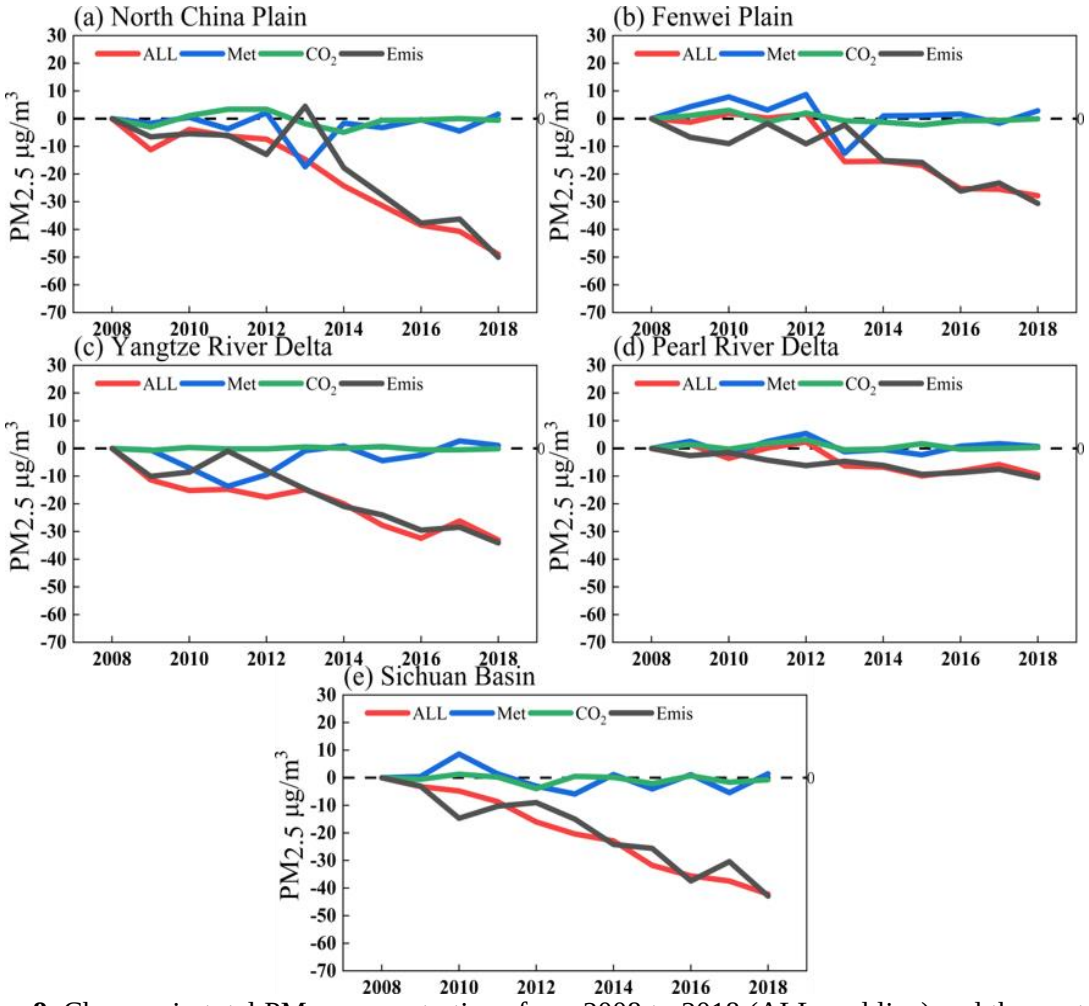

Figure 8. Changes in total $PM_{2.5}$ concentrations from 2008 to 2018 (ALL, red line) and the contributions of anthropogenic pollutant emissions (Emis, black line), meteorological conditions (Met, blue line), and CO_2 emission changes (CO_2, green line) to $PM_{2.5}$ concentrations (Units: $\mu g/m^3$).

3.6 Uncertainties

The uncertainties in the MEIC emission inventory primarily arise from activity data, emission factors, spatial and temporal allocation methods, and the implementation status of pollution control measures (Hong et al., 2017; Zheng et al., 2021b), all of which may affect the accuracy of simulation results. Future improvements can be achieved by employing more refined and accurate emission inventories.

In addition, the use of a 60 km low-resolution grid limits the ability to represent local topography and physical processes, thereby introducing simulation errors (Harris et al., 2016; Ringler et al., 2013). Given that this study employs a fully coupled regional climate-chemistry-ecology model with extended simulation periods (three sets of 10-year simulations) and a broad regional scope (covering the entire East Asia region), computational resource constraints

necessitated the use of 60 km grids. Numerous studies have employed the RegCM-Chem-YIBs model at a 60 km grid resolution to systematically analyze $PM_{2.5}$, O_3, CO_2, and the regional climate over East Asia (Ma et al., 2023a; Ma et al., 2023b; Xu et al., 2023; Gao et al., 2021). These demonstrate its robustness and reliability in simulating East Asian atmospheric and climatic conditions. Future studies could enhance simulation accuracy by increasing computational resources and employing higher-resolution grids.

4 Conclusions

This study employed numerical experiments with the RegCM-Chem-YIBs model to analyze the interannual variability of near-surface $PM_{2.5}$ concentrations in East Asia from 2008 to 2018. The analysis examines the drivers of annual $PM_{2.5}$ changes in detail, focusing on three key factors: anthropogenic pollutant emissions, meteorological conditions, and CO_2 concentration changes.

Compared to 2008, $PM_{2.5}$ concentrations in East Asia exhibited minimal change during the PreG stage, with most areas showing variations between -10 and 5 $\mu g/m^3$. In contrast, following the implementation of the Clean Air Action Plan, $PM_{2.5}$ concentrations decreased significantly during the PostG stage. This reduction was especially notable in the NCP and the SCB region, with declines of 36.76 $\mu g/m^3$ and 33.96 $\mu g/m^3$, respectively.

Anthropogenic pollutant emissions are the primary driver of the decline in $PM_{2.5}$ concentrations in East Asia, with their impact on $PM_{2.5}$ levels increasing linearly over time. During the PreG and PostG stages, the contributions of anthropogenic pollution emissions to $PM_{2.5}$ concentrations in the NCP, FWP, YRD, PRD, and SCB regions ranged from -10.39 to -3.82 $\mu g/m^3$ and -33.86 to -8.45 $\mu g/m^3$, respectively.

Changes in meteorological conditions have led to decreased $PM_{2.5}$ concentrations along China's eastern coastal and western inland regions, while increasing $PM_{2.5}$ levels in central areas. During the PreG stage, the influence of these meteorological changes on $PM_{2.5}$ concentrations was comparable to that of anthropogenic pollution emissions, ranging from -6.31 to 2.32 $\mu g/m^3$.

CO_2 indirectly influences $PM_{2.5}$ concentrations by affecting precipitation and isoprene emissions from vegetation. In the sparsely vegetated NCP and FWP regions, CO_2 impacts near-surface $PM_{2.5}$ primarily through changes in precipitation. Conversely, in the vegetation-rich PRD region, CO_2 affects $PM_{2.5}$ concentrations mainly by altering isoprene emissions, with an impact comparable to that of anthropogenic pollution emissions. From 2009 to 2013, the effects of anthropogenic pollution emissions and CO_2 changes on $PM_{2.5}$ ranged are -0.25 to 3.11 $\mu g/m^3$ and -6.19 to -1.47 $\mu g/m^3$, respectively.

In summary, $PM_{2.5}$ concentrations in East Asia have significantly declined since 2013, primarily driven by changes in anthropogenic pollutant emissions. During several years of the PreG period, variations in meteorological conditions affected $PM_{2.5}$ levels to a degree comparable to that of anthropogenic pollutant emissions. However, following the implementation of the Clean Air Action Plan in 2013, the influence of anthropogenic pollution emissions increased significantly, while the impact of meteorological factors diminished considerably. This simulation underscores the critical importance of stringent air pollution control measures in mitigating $PM_{2.5}$ concentrations. Moreover, we highlight that in regions with dense vegetation cover, changes in CO_2 emissions play a noteworthy role in regulating $PM_{2.5}$ levels, with the average effect during the PostG phase even surpassing that of meteorological conditions. Given the sustained rise in CO_2 levels in recent years, it is imperative to integrate the modulatory effects of CO_2 into $PM_{2.5}$ simulating models and control strategies.

Data availability

ERA-Interim data are available at https://apps.ecmwf.int/datasets/data/interim-full-daily/. MEIC data are available at http://meicmodel.org/?page_id=560. CarbonTracker data are available at https://gml.noaa.gov/aftp/products/carbontracker/co2/CT2019/. WDCGG CO_2 data are available at https://gaw.kishou.go.jp/search/gas_species/co2/latest/. CNEMC data are available at http://www.cnemc.cn/. only available in Chinese, last access 1 August 2024.

Author contributions

MX, TW, and DM: designed the research, and **DM:** carried it out. **MX, and LF:** provided technical support on the RegCM-Chem-YIBs mode. **SZ, and SC:** improved the paper. **HH:** improved and edited the paper.

Competing interests:

The contact author has declared that none of the authors has any competing interests.

Disclaimer

Publisher's note: Copernicus Publications remains neutral with regard to jurisdictional claims in published maps and institutional affiliations.

Financial support

This work was supported by the National Nature Science Foundation of China (grant no. 42275102), the Special Science and Technology Innovation Program for Carbon Peak and Carbon Neutralization of Jiangsu Province (grant no. BE2022612), the research start-up fund for the introduction of talents from Nanjing Normal University (grant no. 184080H201B57), and the Special Science and Technology Innovation Program for Carbon Peak and Carbon Neutralization of Jiangsu Province (BE2022612).

References

Ait-Chaalal, F., Schneider, T., Meyer, B., and Marston, J. B.: Cumulant expansions for atmospheric flows, New Journal of Physics, 18, 10.1088/1367-2630/18/2/025019, 2016.

An, Z. S., Huang, R. J., Zhang, R. Y., Tie, X. X., Li, G. H., Cao, J. J., Zhou, W. J., Shi, Z. G., Han, Y. M., Gu, Z. L., and Ji, Y. M.: Severe haze in northern China: A synergy of anthropogenic emissions and atmospheric processes, P Natl Acad Sci USA, 116, 8657-8666, 10.1073/pnas.1900125116, 2019.

Balsamo, G., Albergel, C., Beljaars, A., Boussetta, S., Brun, E., Cloke, H., Dee, D., Dutra, E., Munoz-Sabater, J., Pappenberger, F., de Rosnay, P., Stockdale, T., and Vitart, F.: ERA-Interim/Land: a global land surface reanalysis data set, Hydrology and Earth System Sciences, 19, 389-407, 10.5194/hess-19-389-2015, 2015.

Bleck, R. and Benjamin, S. G.: REGIONAL WEATHER PREDICTION WITH A MODEL COMBINING TERRAIN-FOLLOWING AND ISENTROPIC COORDINATES .1. MODEL DESCRIPTION, Monthly Weather Review, 121, 1770-1785, 10.1175/1520-0493(1993)121<1770:Rwpwam>2.0.Co;2, 1993.

Cao, L., Bala, G., and Caldeira, K.: Climate response to changes in atmospheric carbon dioxide and solar irradiance on the time scale of days to weeks, Environmental Research Letters, 7, 10.1088/1748-9326/7/3/034015, 2012.

Chen, G. B., Li, S. S., Knibbs, L. D., Hamm, N. A. S., Cao, W., Li, T. T., Guo, J. P., Ren, H. Y., Abramson, M. J., and Guo, Y. M.: A machine learning method to estimate PM_{2.5} concentrations across China with remote sensing, meteorological and land use information, Sci Total Environ, 636, 52-60, 10.1016/j.scitotenv.2018.04.251, 2018.

Chen, L., Zhu, J., Liao, H., Yang, Y., and Yue, X.: Meteorological influences on PM2.5 and O-3 trends and associated health burden since China's clean air actions, Sci Total Environ, 744, 10.1016/j.scitotenv.2020.140837, 2020a.

Chen, Z. Y., Chen, D. L., Zhao, C. F., Kwan, M. P., Cai, J., Zhuang, Y., Zhao, B., Wang, X. Y., Chen, B., Yang, J., Li, R. Y., He, B., Gao, B. B., Wang, K. C., and Xu, B.: Influence of meteorological conditions on PM_{2.5} concentrations across China: A review of methodology and mechanism, Environment International, 139, 10.1016/j.envint.2020.105558, 2020b.

Cheng, J., Su, J. P., Cui, T., Li, X., Dong, X., Sun, F., Yang, Y. Y., Tong, D., Zheng, Y. X., Li, Y. S., Li, J. X., Zhang, Q., and He, K. B.: Dominant role of emission reduction in PM2.5 air quality improvement in Beijing during 2013-2017: a model-based decomposition analysis, Atmospheric Chemistry and Physics, 19, 6125-6146, 10.5194/acp-19-6125-2019, 2019.

Feng, S. L., Gao, D., Liao, F., Zhou, F. R., and Wang, X. M.: The health effects of ambient PM_{2.5} and potential mechanisms, Ecotoxicology and Environmental Safety, 128, 67-74, 10.1016/j.ecoenv.2016.01.030, 2016.

Fontes, T., Li, P. L., Barros, N., and Zhao, P. J.: Trends of PM2.5 concentrations in China: A long term approach, Journal of Environmental Management, 196, 719-732, 10.1016/j.jenvman.2017.03.074, 2017.

Gao, L. B., Wang, T. J., Ren, X. J., Ma, D. Y., Zhuang, B. L., Li, S., Xie, M., Li, M. M., and Yang, X. Q.: Subseasonal characteristics and meteorological causes of surface O-3 in different East Asian summer monsoon periods over the North China Plain during 2014-2019, Atmos Environ, 264, 10.1016/j.atmosenv.2021.118704, 2021.

Geng, G. N., Liu, Y. X., Liu, Y., Liu, S. G., Cheng, J., Yan, L., Wu, N. N., Hu, H. W., Tong, D., Zheng, B., Yin, Z. C., He, K. B., and Zhang, Q.: Efficacy of China's clean air actions to tackle PM_{2.5} pollution between 2013 and 2020, Nature Geoscience, 17, 10.1038/s41561-024-01540-z, 2024.

Harris, L. M., Lin, S. J., and Tu, C. Y.: High-Resolution Climate Simulations Using GFDL HiRAM with a Stretched Global Grid, Journal of Climate, 29, 4293-4314, 10.1175/jcli-d-15-0389.1, 2016.

Heald, C. L., Wilkinson, M. J., Monson, R. K., Alo, C. A., Wang, G. L., and Guenther, A.: Response of isoprene emission to ambient CO2 changes and implications for global budgets, Global Change Biology, 15, 1127-1140, 10.1111/j.1365-2486.2008.01802.x, 2009.

Hong, C. P., Zhang, Q., He, K. B., Guan, D. B., Li, M., Liu, F., and Zheng, B.: Variations of China's emission estimates: response to uncertainties in energy statistics, Atmospheric Chemistry and Physics, 17, 1227-1239, 10.5194/acp-17-1227-2017, 2017.

Hu, B., Zhao, X. J., Liu, H., Liu, Z. R., Song, T., Wang, Y. S., Tang, L. Q., Xia, X. G., Tang, G. Q., Ji, D. S., Wen, T. X., Wang, L. L., Sun, Y., and Xin, J. Y.: Quantification of the impact of aerosol on broadband solar radiation in North China, Sci Rep-Uk, 7, 10.1038/srep44851, 2017.

Huang, B. Y., Liu, C. Y., Banzon, V., Freeman, E., Graham, G., Hankins, B., Smith, T., and Zhang, H. M.: Improvements of the Daily Optimum Interpolation Sea Surface Temperature (DOISST) Version 2.1, Journal of Climate, 34, 2923-2939, 10.1175/jcli-d-20-0166.1, 2021.

Kellomaki, S. and Wang, K. Y.: Growth, respiration and nitrogen content in needles of Scots pine exposed to elevated ozone and carbon dioxide in the field, Environmental pollution (Barking, Essex : 1987), 101, 263-274, 10.1016/s0269-7491(98)00036-0, 1998.

Kergoat, L., Lafont, S., Douville, H., Berthelot, B., Dedieu, G., Planton, S., and Royer, J. F.: Impact of doubled CO₂ on global-scale leaf area index and evapotranspiration:: Conflicting stomatal conductance and LAI responses -: art. no. 4808, Journal of Geophysical Research-Atmospheres, 107, 10.1029/2001jd001245, 2002.

Kim, K. H., Kabir, E., and Kabir, S.: A review on the human health impact of airborne particulate matter, Environment International, 74, 136-143, 10.1016/j.envint.2014.10.005, 2015.

Kleist, E., Mentel, T. F., Andres, S., Bohne, A., Folkers, A., Kiendler-Scharr, A., Rudich, Y., Springer, M., Tillmann, R., and Wildt, J.: Irreversible impacts of heat on the emissions of monoterpenes, sesquiterpenes, phenolic BVOC and green leaf volatiles from several tree species, Biogeosciences, 9, 5111-5123, 10.5194/bg-9-5111-2012, 2012.

Kong, L., Tang, X., Zhu, J., Wang, Z., Li, J., Wu, H., Wu, Q., Chen, H., Zhu, L., Wang, W., Liu, B., Wang, Q., Chen, D., Pan, Y., Song, T., Li, F., Zheng, H., Jia, G., Lu, M., Wu, L., and Carmichael, G. R.: A 6-year-long (2013-2018) high-resolution air quality reanalysis dataset in China based on the assimilation of surface observations from CNEMC, Earth System Science Data, 13, 529-570, 10.5194/essd-13-529-2021, 2021.

Kramer, A. J., Rattanavaraha, W., Zhang, Z. F., Gold, A., Surratt, J. D., and Lin, Y. H.: Assessing the oxidative potential of isoprene-derived epoxides and secondary organic aerosol, Atmos Environ, 130, 211-218, 10.1016/j.atmosenv.2015.10.018, 2016.

Kurokawa, J. and Ohara, T.: Long-term historical trends in air pollutant emissions in Asia: Regional Emission inventory in ASia (REAS) version 3, Atmospheric Chemistry and Physics, 20, 12761-12793, 10.5194/acp-20-12761-2020, 2020.

Lei, Y. D., Yue, X., Liao, H., Gong, C., and Zhang, L.: Implementation of Yale Interactive terrestrial Biosphere model v1.0 into GEOS-Chem v12.0.0: a tool for biosphere-chemistry interactions, Geoscientific Model Development, 13, 1137-1153, 10.5194/gmd-13-1137-2020, 2020.

Li, G. H., Bei, N. F., Cao, J. J., Huang, R. J., Wu, J. R., Feng, T., Wang, Y. C., Liu, S. X., Zhang, Q., Tie, X. X., and Molina, L. T.: A possible pathway for rapid growth of sulfate during haze days in China, Atmospheric Chemistry and Physics, 17, 3301-3316, 10.5194/acp-17-3301-2017, 2017a.

Li, J., Chen, X. S., Wang, Z. F., Du, H. Y., Yang, W. Y., Sun, Y. L., Hu, B., Li, J. J., Wang, W., Wang, T., Fu, P. Q., and Huang, H. L.: Radiative and heterogeneous chemical effects of aerosols on ozone and inorganic aerosols over East Asia, Sci Total Environ, 622, 1327-1342, 10.1016/j.scitotenv.2017.12.041, 2018.

Li, K., Jacob, D. J., Liao, H., Zhu, J., Shah, V., Shen, L., Bates, K. H., Zhang, Q., and Zhai, S. X.: A two-pollutant strategy for improving ozone and particulate air quality in China, Nature Geoscience, 12, 906-+, 10.1038/s41561-019-0464-x, 2019.

Li, X., Feng, Y. J., Liang, H. Y., and Iop: The Impact of Meteorological Factors on PM2.5 Variations in Hong Kong, 8th International Conference on Environmental Science and Technology (ICEST), Technical University Of Madrid, Computer Science School, madrid, SPAIN, Jun 12-14, WOS:000440342600003, 10.1088/1755-1315/78/1/012003, 2017.

Li, Z. and Mölders, N.: Interaction of impacts of doubling CO₂ and changing regional land-cover on evaporation, precipitation, and runoff at global and regional scales, International Journal of Climatology, 28, 1653-1679, 10.1002/joc.1666, 2008.

Lin, C. Q., Liu, G., Lau, A. K. H., Li, Y., Li, C. C., Fung, J. C. H., and Lao, X. Q.: High-resolution satellite remote sensing of provincial PM_{2.5} trends in China from 2001 to 2015, Atmos Environ, 180, 110-116, 10.1016/j.atmosenv.2018.02.045, 2018.

Lin, Y. H., Knipping, E. M., Edgerton, E. S., Shaw, S. L., and Surratt, J. D.: Investigating the influences of SO₂ and NH₃ levels on isoprene-derived secondary organic aerosol formation using conditional sampling approaches, Atmospheric Chemistry and Physics, 13, 8457-8470, 10.5194/acp-13-8457-2013, 2013.

Lindwall, F., Schollert, M., Michelsen, A., Blok, D., and Rinnan, R.: Fourfold higher tundra volatile emissions due to arctic summer warming, Journal of Geophysical Research-Biogeosciences, 121, 895-902, 10.1002/2015jg003295, 2016.

Ma, D., Wang, T., Wu, H., Qu, Y., Liu, J., Liu, J., Li, S., Zhuang, B., Li, M., and Xie, M.: The effect of anthropogenic emission, meteorological factors, and carbon dioxide on the surface ozone increase in China from 2008 to 2018 during the East Asia summer monsoon season, Atmos. Chem. Phys., 23, 6525-6544, 10.5194/acp-23-6525-2023, 2023a.

671 Ma, D. Y., Wang, T. J., Xu, B. Y., Song, R., Gao, L. B., Chen, H. M., Ren, X. J., Li, S., Zhuang, B. L., Li, M. M., Xie,
672 M., and Saikawa, E.: The mutual interactions among ozone, fine particulate matter, and carbon dioxide on
673 summer monsoon climate in East Asia, Atmos Environ, 299, 10.1016/j.atmosenv.2023.119668, 2023b.
674 Ma, Z., Liu, R., Liu, Y., and Bi, J.: Effects of air pollution control policies on PM_{2.5} pollution
675 improvement in China from 2005 to 2017: a satellite-based perspective, Atmospheric Chemistry and
676 Physics, 19, 6861-6877, 10.5194/acp-19-6861-2019, 2019.
677 Ma, Z. W., Hu, X. F., Sayer, A. M., Levy, R., Zhang, Q., Xue, Y. G., Tong, S. L., Bi, J., Huang, L., and Liu, Y.:
678 Satellite-Based Spatiotemporal Trends in PM2.5 Concentrations: China, 2004-2013, Environmental Health
679 Perspectives, 124, 184-192, 10.1289/ehp.1409481, 2016.
680 Matthews, H. D.: Implications of CO₂ fertilization for future climate change in a coupled climate-
681 carbon model, Global Change Biology, 13, 1068-1078, 10.1111/j.1365-2486.2007.01343.x, 2007.
682 Mousavinezhad, S., Choi, Y., Pouyaei, A., Ghahremanloo, M., and Nelson, D. L.: A comprehensive investigation of
683 surface ozone pollution in China, 2015-2019: Separating the contributions from meteorology and precursor
684 emissions, Atmospheric Research, 257, 10.1016/j.atmosres.2021.105599, 2021.
685 Pan, L., Xu, J. M., Tie, X. X., Mao, X. Q., Gao, W., and Chang, L. Y.: Long-term measurements of planetary
686 boundary layer height and interactions with PM_{2.5} in Shanghai, China, Atmospheric Pollution
687 Research, 10, 989-996, 10.1016/j.apr.2019.01.007, 2019.
688 Pegoraro, E., Rey, A., Bobich, E. G., Barron-Gafford, G., Grieve, K. A., Malhi, Y., and Murthy, R.: Effect of
689 elevated CO₂ concentration and vapour pressure deficit on isoprene emission from leaves of
690 Populus deltoides during drought, Functional Plant Biology, 31, 1137-1147,
691 10.1071/fp04142, 2004.
692 Peters, W., Jacobson, A. R., Sweeney, C., Andrews, A. E., Conway, T. J., Masarie, K., Miller, J. B., Bruhwiler, L. M.
693 P., Petron, G., Hirsch, A. I., Worthy, D. E. J., van der Werf, G. R., Randerson, J. T., Wennberg, P. O., Krol,
694 M. C., and Tans, P. P.: An atmospheric perspective on North American carbon dioxide exchange:
695 CarbonTracker, P Natl Acad Sci USA, 104, 18925-18930, 10.1073/pnas.0708986104, 2007.
696 Possell, M., Hewitt, C. N., and Beerling, D. J.: The effects of glacial atmospheric CO2 concentrations and climate on
697 isoprene emissions by vascular plants, Global Change Biology, 11, 60-69, 10.1111/j.1365-
698 2486.2004.00889.x, 2005.
699 Pui, D. Y. H., Chen, S. C., and Zuo, Z. L.: PM2.5 in China: Measurements, sources, visibility and health effects, and
700 mitigation, Particuology, 13, 1-26, 10.1016/j.partic.2013.11.001, 2014.
701 Ringler, T., Petersen, M., Higdon, R. L., Jacobsen, D., Jones, P. W., and Maltrud, M.: A multi-resolution approach to
702 global ocean modeling, Ocean Modelling, 69, 211-232, 10.1016/j.ocemod.2013.04.010, 2013.
703 Shalaby, A., Zakey, A. S., Tawfik, A. B., Solmon, F., Giorgi, F., Stordal, F., Sillman, S., Zaveri, R. A., and Steiner, A.
704 L.: Implementation and evaluation of online gas-phase chemistry within a regional climate model (RegCM-
705 CHEM4), Geoscientific Model Development, 5, 741-760, 10.5194/gmd-5-741-2012, 2012.
706 Silver, B., Reddington, C. L., Arnold, S. R., and Spracklen, D. V.: Substantial changes in air pollution across China
707 during 2015-2017, Environmental Research Letters, 13, 10.1088/1748-9326/aae718, 2018.
708 Silver, B., Reddington, C. L., Chen, Y., and Arnold, S. R.: A decade of China's air quality monitoring data suggests
709 health impacts are no longer declining, Environment International, 197, 10.1016/j.envint.2025.109318,
710 2025.
711 Sun, Z. H., Hve, K., Vislap, V., and Niinemets, U.: Elevated CO2 magnifies isoprene emissions under heat and
712 improves thermal resistance in hybrid aspen, Journal of Experimental Botany, 64, 5509-5523,
713 10.1093/jxb/ert318, 2013.
714 Sun, Z. H., Niinemets, Ü., Hüve, K., Noe, S. M., Rasulov, B., Copolovici, L., and Vislap, V.: Enhanced isoprene
715 emission capacity and altered light responsiveness in aspen grown under elevated atmospheric CO2
716 concentration, Global Change Biology, 18, 3423-3440, 10.1111/j.1365-2486.2012.02789.x, 2012.
717 van Donkelaar, A., Martin, R. V., Li, C., and Burnett, R. T.: Regional Estimates of Chemical Composition of Fine
718 Particulate Matter Using a Combined Geoscience-Statistical Method with Information from Satellites,
719 Models, and Monitors, Environmental Science & Technology, 53, 2595-2611, 10.1021/acs.est.8b06392,
720 2019.
721 van Donkelaar, A., Martin, R. V., Brauer, M., Kahn, R., Levy, R., Verduzco, C., and Villeneuve, P. J.: Global
722 Estimates of Ambient Fine Particulate Matter Concentrations from Satellite-Based Aerosol Optical Depth:
723 Development and Application, Environmental Health Perspectives, 118, 847-855, 10.1289/ehp.0901623,
724 2010.
725 Vu, T. V., Shi, Z. B., Cheng, J., Zhang, Q., He, K. B., Wang, S. X., and Harrison, R. M.: Assessing the impact of
726 clean air action on air quality trends in Beijing using a machine learning technique, Atmospheric Chemistry

727 and Physics, 19, 11303-11314, 10.5194/acp-19-11303-2019, 2019.
728 Wang, H., Peng, Y., Zhang, X. Y., Liu, H. L., Zhang, M., Che, H. Z., Cheng, Y. L., and Zheng, Y.: Contributions to
729 the explosive growth of PM2.5 mass due to aerosol-radiation feedback and decrease in turbulent diffusion
730 during a red alert heavy haze in Beijing-Tianjin-Hebei, China, Atmospheric Chemistry and Physics, 18,
731 17717-17733, 10.5194/acp-18-17717-2018, 2018a.
732 Wang, H. B., Tian, M., Chen, Y., Shi, G. M., Liu, Y., Yang, F. M., Zhang, L. M., Deng, L. Q., Yu, J., Peng, C., and
733 Cao, X. Y.: Seasonal characteristics, formation mechanisms and source origins of PM_{2.5} in
734 two megacities in Sichuan Basin, China, Atmospheric Chemistry and Physics, 18, 865-881, 10.5194/acp-
735 18-865-2018, 2018b.
736 Wang, J. D., Zhao, B., Wang, S. X., Yang, F. M., Xing, J., Morawska, L., Ding, A. J., Kulmala, M., Kerminen, V. M.,
737 Kujansuu, J., Wang, Z. F., Ding, D. A., Zhang, X. Y., Wang, H. B., Tian, M., Petaja, T., Jiang, J. K., and
738 Hao, J. M.: Particulate matter pollution over China and the effects of control policies, Sci Total Environ,
739 584, 426-447, 10.1016/j.scitotenv.2017.01.027, 2017.
740 Wei, J., Li, Z. Q., Lyapustin, A., Sun, L., Peng, Y. R., Xue, W. H., Su, T. N., and Cribb, M.: Reconstructing 1-km-
741 resolution high-quality PM2.5 data records from 2000 to 2018 in China: spatiotemporal variations and
742 policy implications, Remote Sens Environ, 252, ARTN 112136
743 10.1016/j.rse.2020.112136, 2021.
744 Wilkinson, M. J., Monson, R. K., Trahan, N., Lee, S., Brown, E., Jackson, R. B., Polley, H. W., Fay, P. A., and Fall,
745 R.: Leaf isoprene emission rate as a function of atmospheric CO2 concentration, Global Change Biology,
746 15, 1189-1200, 10.1111/j.1365-2486.2008.01803.x, 2009.
747 Wu, H., Wang, T. J., Wang, Q., Cao, Y., Qu, Y. W., and Nie, D. Y.: Radiative effects and chemical compositions of
748 fine particles modulating urban heat island in Nanjing, China, Atmos Environ, 247,
749 10.1016/j.atmosenv.2021.118201, 2021.
750 Wu, K., Yang, X. Y., Chen, D., Gu, S., Lu, Y. Q., Jiang, Q., Wang, K., Ou, Y. H., Qian, Y., Shao, P., and Lu, S. H.:
751 Estimation of biogenic VOC emissions and their corresponding impact on ozone and secondary organic
752 aerosol formation in China, Atmospheric Research, 231, 10.1016/j.atmosres.2019.104656, 2020.
753 Wu, Y. N., Liu, J. K., Zhai, J. X., Cong, L., Wang, Y., Ma, W. M., Zhang, Z. M., and Li, C. Y.: Comparison of dry
754 and wet deposition of particulate matter in near-surface waters during summer, Plos One, 13,
755 10.1371/journal.pone.0199241, 2018.
756 Xiao, Q. Y., Zheng, Y. X., Geng, G. N., Chen, C. H., Huang, X. M., Che, H. Z., Zhang, X. Y., He, K. B., and Zhang,
757 Q.: Separating emission and meteorological contributions to long-term PM_{2.5} trends over
758 eastern China during 2000-2018, Atmospheric Chemistry and Physics, 21, 9475-9496, 10.5194/acp-21-
759 9475-2021, 2021.
760 Xie, N. H., Wang, T. J., Xie, X. D., Yue, X., Giorgi, F., Zhang, Q., Ma, D. Y., Song, R., Xu, B. Y., Li, S., Zhuang, B.
761 L., Li, M. M., Xie, M., Kilifarska, N. A., Gadzhev, G., and Dimitrova, R.: The regional climate-chemistry-
762 ecology coupling model RegCM-Chem (v4.6)-YIBs (v1.0): development and application, Geoscientific
763 Model Development, 17, 3259-3277, 10.5194/gmd-17-3259-2024, 2024.
764 Xie, X., Wang, T., Yue, X., Li, S., Zhuang, B., Wang, M., and Yang, X.: Numerical modeling of ozone damage to
765 plants and its effects on atmospheric CO2 in China, Atmospheric Environment, 217,
766 10.1016/j.atmosenv.2019.116970, 2019.
767 Xing, Y. F., Xu, Y. H., Shi, M. H., and Lian, Y. X.: The impact of PM2.5 on the human respiratory system, Journal of
768 Thoracic Disease, 8, E69-E74, 10.3978/j.issn.2072-1439.2016.01.19, 2016.
769 Xu, B. Y., Wang, T. J., Ma, D. Y., Song, R., Zhang, M., Gao, L. B., Li, S., Zhuang, B. L., Li, M. M., and Xie, M.:
770 Impacts of regional emission reduction and global climate change on air quality and temperature to attain
771 carbon neutrality in China, Atmospheric Research, 279, 10.1016/j.atmosres.2022.106384, 2022.
772 Xu, B. Y., Wang, T. J., Gao, L. B., Ma, D. Y., Song, R., Zhao, J., Yang, X. G., Li, S., Zhuang, B. L., Li, M. M., and
773 Xie, M.: Impacts of meteorological factors and ozone variation on crop yields in China concerning carbon
774 neutrality objectives in 2060, Environmental Pollution, 317, 10.1016/j.envpol.2022.120715, 2023.
775 Xue, W. H., Zhang, J., Zhong, C., Ji, D. Y., and Huang, W.: Satellite-derived spatiotemporal PM2.5 concentrations
776 and variations from 2006 to 2017 in China, Sci Total Environ, 712, 10.1016/j.scitotenv.2019.134577, 2020.
777 Yue, X. and Unger, N.: The Yale Interactive terrestrial Biosphere model version 1.0: description, evaluation and
778 implementation into NASA GISS ModelE2, Geoscientific Model Development, 8, 2399-2417,
779 10.5194/gmd-8-2399-2015, 2015.
780 Yue, X., Unger, N., and Zheng, Y.: Distinguishing the drivers of trends in land carbon fluxes and plant volatile
781 emissions over the past 3 decades, Atmospheric Chemistry and Physics, 15, 11931-11948, 10.5194/acp-15-
782 11931-2015, 2015.

783 Zhai, S. X., Jacob, D. J., Wang, X., Shen, L., Li, K., Zhang, Y. Z., Gui, K., Zhao, T. L., and Liao, H.: Fine particulate
784 matter (PM2.5) trends in China, 2013-2018: separating contributions from anthropogenic emissions and
785 meteorology, Atmospheric Chemistry and Physics, 19, 11031-11041, 10.5194/acp-19-11031-2019, 2019.
786 Zhang, B. E., Jiao, L. M., Xu, G., Zhao, S. L., Tang, X., Zhou, Y., and Gong, C.: Influences of wind and
787 precipitation on different-sized particulate matter concentrations (PM_{2.5}, PM₁₀,
788 PM_{2.5-10}), Meteorol Atmos Phys, 130, 383-392, 10.1007/s00703-017-0526-9, 2018.
789 Zhang, Q., Zheng, Y. X., Tong, D., Shao, M., Wang, S. X., Zhang, Y. H., Xu, X. D., Wang, J. N., He, H., Liu, W. Q.,
790 Ding, Y. H., Lei, Y., Li, J. H., Wang, Z. F., Zhang, X. Y., Wang, Y. S., Cheng, J., Liu, Y., Shi, Q. R., Yan, L.,
791 Geng, G. N., Hong, C. P., Li, M., Liu, F., Zheng, B., Cao, J. J., Ding, A. J., Gao, J., Fu, Q. Y., Huo, J. T., Liu,
792 B. X., Liu, Z. R., Yang, F. M., He, K. B., and Hao, J. M.: Drivers of improved PM2.5 air quality in China
793 from 2013 to 2017, P Natl Acad Sci USA, 116, 24463-24469, 10.1073/pnas.1907956116, 2019.
794 Zhang, Y., Olsen, K. M., and Wang, K.: Fine Scale Modeling of Agricultural Air Quality over the Southeastern
795 United States Using Two Air Quality Models. Part I. Application and Evaluation, Aerosol and Air Quality
796 Research, 13, 1231-1252, 10.4209/aaqr.2012.12.0346, 2013.
797 Zhang, Y., Gentine, P., Luo, X. Z., Lian, X., Liu, Y. L., Zhou, S., Michalak, A. M., Sun, W., Fisher, J. B., Piao, S. L.,
798 and Keenan, T. F.: Increasing sensitivity of dryland vegetation greenness to precipitation due to rising
799 atmospheric CO₂, Nature Communications, 13, 10.1038/s41467-022-32631-3, 2022.
800 Zheng, B., Zhang, Q., Geng, G. N., Chen, C. H., Shi, Q. R., Cui, M. S., Lei, Y., and He, K. B.: Changes in China's
801 anthropogenic emissions and air quality during the COVID-19 pandemic in 2020, Earth System Science
802 Data, 13, 2895-2907, 10.5194/essd-13-2895-2021, 2021a.
803 Zheng, B., Cheng, J., Geng, G. N., Wang, X., Li, M., Shi, Q. R., Qi, J., Lei, Y., Zhang, Q., and He, K. B.: Mapping
804 anthropogenic emissions in China at 1 km spatial resolution and its application in air quality modeling,
805 Science Bulletin, 66, 612-620, 10.1016/j.scib.2020.12.008, 2021b.
806 Zheng, B., Tong, D., Li, M., Liu, F., Hong, C. P., Geng, G. N., Li, H. Y., Li, X., Peng, L. Q., Qi, J., Yan, L., Zhang, Y.
807 X., Zhao, H. Y., Zheng, Y. X., He, K. B., and Zhang, Q.: Trends in China's anthropogenic emissions since
808 2010 as the consequence of clean air actions, Atmospheric Chemistry and Physics, 18, 14095-14111,
809 10.5194/acp-18-14095-2018, 2018.
810 Zhong, J. T., Zhang, X. Y., Dong, Y. S., Wang, Y. Q., Liu, C., Wang, J. Z., Zhang, Y. M., and Che, H. C.: Feedback
811 effects of boundary-layer meteorological factors on cumulative explosive growth of PM_{2.5}
812 during winter heavy pollution episodes in Beijing from 2013 to 2016, Atmospheric Chemistry and Physics,
813 18, 247-258, 10.5194/acp-18-247-2018, 2018.
814